Mathematical Modeling and Dynamic Simulation of the Nerinjipettai Hydropower Plant Using MATLAB/Simulink

D. Santhosh Kumar
Department of Mechatronics, School of Mechanical Engineering, SRM Institute of Science and Technology, Chennai, Tamil Nadu, India | Department of Electrical and Electronics Engineering, Vivekanandha College of Engineering for Women, Namakkal, India
sd4136@srmist.edu.in (corresponding author)

V. Sujatha
Department of Mechatronics, School of Mechanical Engineering, SRM Institute of Science and Technology, Chennai, Tamil Nadu, India
sujathav2@srmist.edu.in

Received: 1 August 2025 | Revised: 17 September 2025, 13 October 2025, and 27 October 2025 | Accepted: 29 October 2025

 DOI: https://doi.org/10.48084/etasr.13766

ABSTRACT

Micro-hydroelectric power is a reliable and efficient source of clean and renewable energy. It can be a fully sustainable method for generating renewable energy from small rivers and streams. The micro-hydro project is designed as a run-of-river system with only a tiny reservoir to operate the turbine, and the water returns to the stream for other purposes without causing significant ecological impact. In this study, a comprehensive MATLAB/Simulink model was developed for the Nerinjipettai Hydropower Plant, incorporating the hydraulic turbine, governor, synchronous generator, and excitation system. A three-phase-to-ground fault was simulated at the generator terminals, where the results showed a terminal voltage dip of about 10% with recovery in 0.6 s, a rotor speed deviation of around 2% that settled within 1.5 s, and mechanical power restored without steady-state error. The novelty of this work lies in integrating plant-specific features of Nerinjipettai with detailed transient fault analysis, which is rarely addressed in previous hydropower modeling studies. The proposed model demonstrates reliable dynamic performance, with the governor and excitation system ensuring system stability. These findings can be applied to optimize control strategies and enhance the efficiency and stability of real-world hydroelectric plants.

Keywords-renewable energy systems; hydropower modeling; MATLAB/Simulink modeling; Kaplan turbine; three-phase fault analysis; transient stability

I. INTRODUCTION

Electricity demand has been increasing rapidly in recent years, while fossil fuel-based generation remains a leading contributor to environmental pollution [1]. To address this challenge, renewable energy sources have become a global priority [2]. Among these, hydropower is considered one of the most sustainable and reliable options for clean energy production [3]. The basic principle of hydropower involves converting the potential energy of falling water into mechanical energy through turbines, which is then transformed into electrical power by a generator [4]. The overall system configuration is illustrated in Figure 1, which presents the block diagram of a hydropower plant including the turbine, generator, excitation system, and control loops.

However, the adoption of hydropower is often constrained by geographical and economic challenges, such as the requirement for sufficient water flow and elevation difference, high capital investment, and maintenance in remote areas. Addressing these limitations is crucial for its sustainable expansion. Hydropower plants are generally categorized into storage type, pumped-storage type, and run-of-river type [5]. The present study focuses on a run-of-river system, specifically the Nerinjipettai Hydropower Plant in Tamil Nadu, India, which has an installed capacity of 30 MW and operates with Kaplan turbines. These practical details provide context for the proposed simulation model.

The unique contribution of this work lies in developing a plant-specific MATLAB/Simulink dynamic model that integrates the hydraulic turbine, governor, synchronous generator, and excitation system, validated using operational

data from the Nerinjipettai plant. Unlike previous studies that primarily address generic or idealized configurations [6-12], this work emphasizes transient fault response analysis and realistic system validation, providing insights into system reliability and control performance under disturbance conditions. The control system plays a vital role in ensuring stability, particularly during load variations or electrical faults. In this study, a Proportional-Integral-Derivative (PID) controller is implemented for turbine speed regulation, and an Automatic Voltage Regulator (AVR) ensures generator terminal voltage stability. These controllers jointly support transient stability by damping oscillations and restoring steady-state conditions.

Recent works in hydropower modeling, renewable integration, and advanced control have reinforced the relevance of simulation-based studies. For instance, authors in [13-17] discuss advancements in control design, renewable integration, and transient stability modeling. Compared to these approaches, the present study provides a validated case-specific framework that captures low-head hydropower dynamics under real operating and fault conditions, thereby extending existing research on dynamic performance analysis of run-of-river installations.

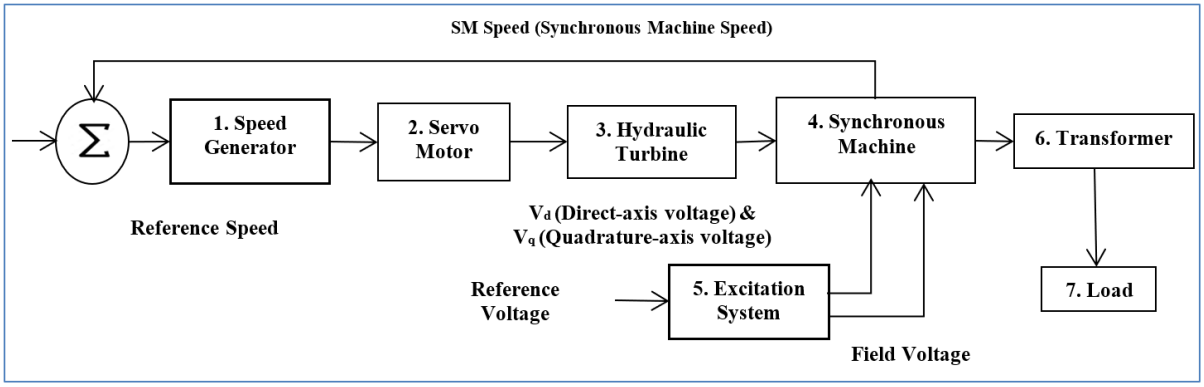

Fig. 1. Block diagram of a hydropower plant system.

II. SYSTEM MODELING

A. Hydro Turbine

These turbine generators are built with a horizontal-axis propeller with adjustable blades, enclosed in a bulb-shaped casing that guides the water flow efficiently. In this design, known as a bulb turbine, water flows around the central bulb and into the generator, ensuring smooth operation. It functions as a horizontal Kaplan reaction turbine, suitable for low-head applications ranging from 2 m to 20 m [15, 16].

The transient performance of a hydraulic turbine is calculated based on the assumptions:

1. The frictional resistance of the turbine blade is disregarded because they are assumed to be smooth.
2. Water hammer effects in the penstock must be considered; however, the fluid is treated as incompressible, and a direct correlation is assumed between gate opening and water velocity in the penstock.

The system's behavior is defined in terms of gate opening and net head, expressed as functions of flow rate and mechanical power at the turbine shaft:

$$Q = G\sqrt{H} \quad (1)$$

where G denotes the gate opening, Q denotes the flow rate, and H denotes the pressure head. Therefore, the developed power P_m is given by:

$$P_m = A_t H(Q - Q_{nl}) \quad (2)$$

where A_t and Q_{nl} are the turbine gain and the no-flow rate, respectively. Here, $A_t = 1/g_{FL} - g_{NL}$, where g_{FL} and g_{NL} denote the full load and no-load gate openings, respectively.

The penstock water flow can be described as:

$$U = K_u G\sqrt{H} \quad (3)$$

Here, U denotes the water velocity, and K_u is a proportional constant. With the water velocity determined, the flow rate and net head can be expressed as:

$$Q = AU \quad (4)$$

The fluid in the penstock accelerates, and its acceleration is described by:

$$\frac{dU}{dt} = -\frac{a_g}{L}(H - H_0) \quad (5)$$

Here, a_g denotes the gravitational acceleration, and L denotes the penstock length. The pressure head is given by:

$$H = \left(\frac{U}{G}\right)^2 \quad (6)$$

B. Hydro Turbine Governing System

A micro-hydropower plant contains both mechanical and electrical sections. The mechanical section includes components such as penstock, controller, hydraulic servomotor, regulating valve, and hydraulic turbine. The electrical section includes a generator and a load that operate together to provide the preferred output. The hydro turbine governor is a crucial

component of the plant that combines a hydroelectric servomotor, controller, and hydraulic turbine. The torque and turbine flow are expressed as:

$$M_t = M_t(y, H, \omega) \quad (7)$$

$$Q = Q(y, H, \omega) \quad (8)$$

$$q = e_{qy}y + e_{qx}x + e_q h \quad (9)$$

$$M = e_y y + e_x x + e_h h \quad (10)$$

$$e_y = \frac{\partial M_t}{\partial y}, \text{Torque sensitivity to gate opening} \quad (11)$$

$$e_x = \frac{\partial M_t}{\partial x}, \text{Torque sensitivity to turbine speed} \quad (12)$$

$$e_h = \frac{\partial M_t}{\partial h}, \text{Torque sensitivity to turbine head} \quad (13)$$

$$e_{qx} = \frac{\partial q}{\partial x}, \text{Flow sensitivity to turbine speed} \quad (14)$$

$$e_{qy} = \frac{\partial q}{\partial y}, \text{Flow sensitivity to gate opening} \quad (15)$$

$$e_{qh} = \frac{\partial q}{\partial h}, \text{Flow sensitivity to turbine head} \quad (16)$$

where M_t denotes the mechanical torque in N·m, y is the gate opening, Q is the flow rate, H is the pressure head, ω is the angular speed in rad/s, q denotes the turbine flow (p.u.), h denotes the turbine head at turbine admission, L denotes the conduit length, and g is the gravitational acceleration.

This chapter presents the mathematical modeling of the hydro turbine governor, focusing on equations that describe flow and mechanical power variations based on turbine speed, gate position, and runner blade movement. The Kaplan turbine, an inward-flow reaction type, generates power as water flows through it under varying pressure conditions.

C. Controller Model

The PID controller is proven to be more effective than other methods in damping power oscillations after load changes [16, 17]. It minimizes the speed error between actual and reference values. The controller uses Proportional (P), Integral (I), and Derivative (D) actions to adjust the output based on the velocity error:

$$\theta(t) = k_p e(t) + k_i \int e(t)\, dt + k_d \frac{de(t)}{dt} \quad (17)$$

Taking the Laplace transform on both sides:

$$\theta(s) = k_p E(s) + \frac{k_i}{s} E(s) + k_d s E(s) \quad (18)$$

Therefore, the transfer function can be expressed as:

$$C(s) = \frac{\theta(s)}{E(s)} = k_p + \frac{k_i}{s} + k_d s \quad (19)$$

D. Servo Motor Model

A servo motor operates the gate valve in the hydro turbine governor model in response to controller signals, which negates the speed signal inaccuracy. The motor torque is a function of rotor position and error signal:

$$T_m = f(\theta, e) \quad (20)$$

The servo motor torque equation can be expressed using Taylor's series:

$$T_m = T_m(0) + \frac{\partial T_m}{\partial e}\big(e(t) - e(0)\big) + \frac{\partial T_m}{\partial \theta}\big(\theta(t) - \theta(0)\big) + \cdots \quad (21)$$

Taking zero initial conditions into consideration and ignoring higher-order terms:

$$T_m = k_e e(t) - f\theta(t) \quad (22)$$

where:

$$k_e = \frac{dT_m}{de}, \; f = -\frac{dT_m}{d\theta} \quad (23)$$

The mechanical relation of the synchronous motor is expressed as:

$$T_m = B\theta' + J\theta'' \quad (24)$$

Here, J and B are the moment of inertia and viscous friction coefficient, respectively. Therefore:

$$k_e e(t) - f\theta(t) = B\theta' + J\theta'' \quad (25)$$

Taking the Laplace transform:

$$\frac{\Theta(s)}{E(s)} = \frac{k_e}{Js^2 + Bs + f} \quad (26)$$

E. Model of Synchronous Machine

Synchronous generators play a vital role in the final stage of power generation in hydroelectric plants. As the turbine rotates, it drives the rotor, producing electrical energy [18]. The synchronous machine model helps analyze both mechanical and electrical behavior, including the dynamics of stator, field, and damper windings. Electrical parameters are represented using primed variables. The model assumes that currents flow through the stator windings and exit the machine [19, 20]. A controller regulates the valve via a servo motor, correcting any speed deviations. The corresponding mathematical expressions are:

$$T'_{d0} \frac{dE''_q}{dt} = E'_q - E''_q - (X'_d - X''_d) I_d \quad (27)$$

$$T'_{q0} \frac{dE''_d}{dt} = E'_d - E''_d + \big(X'_q - X''_q\big) I_q \quad (28)$$

$$T'_{d0} \frac{dE'_q}{dt} = E_f - E'_q - (X'_d - X''_d) I_d \quad (29)$$

$$T'_{q0} \frac{dE'_d}{dt} = -E'_d + \big(X'_q - X''_q\big) I_q \quad (30)$$

Table I summarizes the key symbols and their corresponding units used in the mathematical modeling presented above for clarity and ease of reference.

III. NERINJIPETTAI PLANT OVERVIEW

The Nerinjipettai Hydropower Plant is a run-of-river barrage-based facility with an installed capacity of 30 MW (2 × 15 MW units), located on the Kaveri River in Tamil Nadu, India. It was developed to support regional grid stability and peak demand management using low-head bulb turbines, which operate efficiently under variable flow conditions. The plant is part of the broader Mettur hydropower system, which includes

the Tunnel Powerhouse (200 MW) and the Dam Powerhouse (40 MW), as well as a series of barrages: Bhavani Katalin, Uratchi Kottai, Koneripatti, Nerinjipettai, and Chekkanur. These barrages are installed along the river. The Mettur Dam, constructed between 1934 and 1943 across the Kaveri River, creates the Stanley Reservoir and supplies water to these facilities. It stands 214 ft high and 171 ft wide with a maximum storage height of 120 ft, receiving inflow from the Krishna Raja Sagara and Kabini dams in Karnataka. In this study, the Nerinjipettai barrage channels water to a bulb turbine-driven powerhouse. Its operating parameters, shown in Table II, were used for model development and validation. The schematic layout of the Nerinjipettai Hydropower Plant is shown in Figure 2.

TABLE I. SYMBOLS AND NOTATIONS

S. No	Symbol	Meaning	Unit
1	H	Hydraulic head (net head)	m
2	H_0	Reference/static head	m
3	g	Gravitational acceleration	m/s²
4	L	Penstock length	m
5	Q	Turbine/penstock flow rate	m³/s
6	A	Cross-sectional area of conduit	m²
7	G	Gate opening	pu
8	k_p, k_i, k_d	Controller gains (PID)	-
9	$e(t)$	Control error signal	-
10	$\theta(t)$	Controller output	-
11	$E(s)$	Laplace transform of e(t)	-
12	$C(s)$	PID transfer function	-
13	θ	Rotor angular position	rad
14	θ'	Rotor angular speed	rad/s
15	θ''	Rotor angular acceleration	rad/s²
16	J	Total rotor inertia	kg·m²
17	B	Viscous damping coefficient	N·m·s/rad
18	T_m	Mechanical input torque	N·m

TABLE II. TURBINE PARAMETERS OF NERINJIPETTAI HYDROPOWER PLANT

S. No	Term	Parameters / values	Unit
1	Type	Bulb turbine	-
2	Net head(minimum / rated / maximum)	6.50 / 7.53 / 30	m
3	Speed	75.00	RPM
4	Runaway speed	205.00	RPM
5	Runner motor	Servo (1)	-
6	Runner flow (minimum / rated / maximum)	182.60 / 253.10 / 271.00	m^3/s
7	Water level downstream	184.25	m

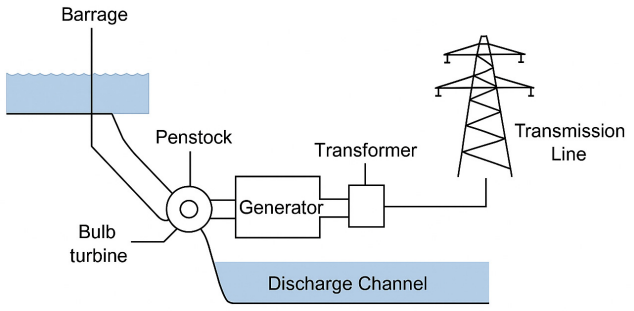

Fig. 2. Simplified schematic of the Nerinjipettai Hydropower Plant showing the actual plant layout and main components.

IV. SIMULINK MODEL SETUP

The hydropower plant is modeled in MATLAB/Simulink for dynamic analysis. A 200 MVA salient-pole synchronous generator operating at 13.8 kV and 50 Hz is connected to a 230 kV grid through a 210 MVA delta-Y transformer. A hydraulic turbine with governor supplies mechanical input, while a DC system supplies excitation. The model includes a 10 MW load and a three-phase ground fault. The model uses the "PV Generator" configuration in PowerGUI to regulate power and terminal voltage [19, 20]. A PID controller regulates gate flow based on rotor speed deviation, whereas a regulating transformer stabilizes the high-voltage side. The governor parameters used in the simulation were: permanent droop = 0.05 pu, proportional gain = 1.163, integral gain = 0.105, derivative gain = 0.01, and servo-motor time constant = 0.07 s. Figure 3 shows the MATLAB/Simulink model of the hydropower plant with a three-phase-to-ground fault.

The chosen parameters, such as generator rating, transformer capacity, and fault conditions, were based on values commonly reported in hydropower plant studies, ensuring realistic operating conditions. The simulation was implemented in MATLAB/Simulink R2023a using the Simscape Electrical and Simscape Fluids toolboxes for detailed electrical and hydraulic subsystem modeling [21-23]. A fixed sampling time of 50 µs was adopted to capture fast transients, and the system was executed in continuous mode with the ODE solver, suitable for stiff power system models. An ideal sensor feedback assumption was employed to focus the analysis on the dynamic response of the plant and control system. These configurations ensure clarity, reproducibility, and alignment with current hydropower simulation practices.

V. RESULTS AND DISCUSSION

The simulation was performed in generating mode for 2 s. A three-phase-to-ground fault was applied to the synchronous generator terminals at t = 0.8 s and cleared at t = 0.92 s. Figures 4–7 show how rotor speed, excitation voltage, mechanical power, and terminal voltage deviate during the fault and return to normal afterward, highlighting the model's ability to capture both transient and steady-state behaviors.

The main transient occurs between 0.8 and 1.0 s, after which the system recovers to the steady state. Rotor speed shows a deviation of approximately 2% and settles within about 1.5 s. Terminal voltage dips by about 10% during the fault and recovers within 0.6 s. Mechanical power falls by around 8% but is fully restored with no steady-state error. The excitation system responds quickly with a temporary boost in field voltage, stabilizing within 1.2 s. These dynamic ranges are consistent with reported values for Kaplan turbine-based run-of-river hydro units, in which speed typically settles in 1 to 3 s and terminal voltage recovers in less than 1 s following short-duration faults. This confirms that the simulated model reflects practical hydro unit behavior. Baseline studies of similar hydro units report rotor speed deviations of 2–3% and voltage recovery within 1 s. The present model aligns with these benchmarks while achieving a slightly faster settling time (0.6 s for voltage recovery), highlighting its reliability in capturing practical system dynamics.

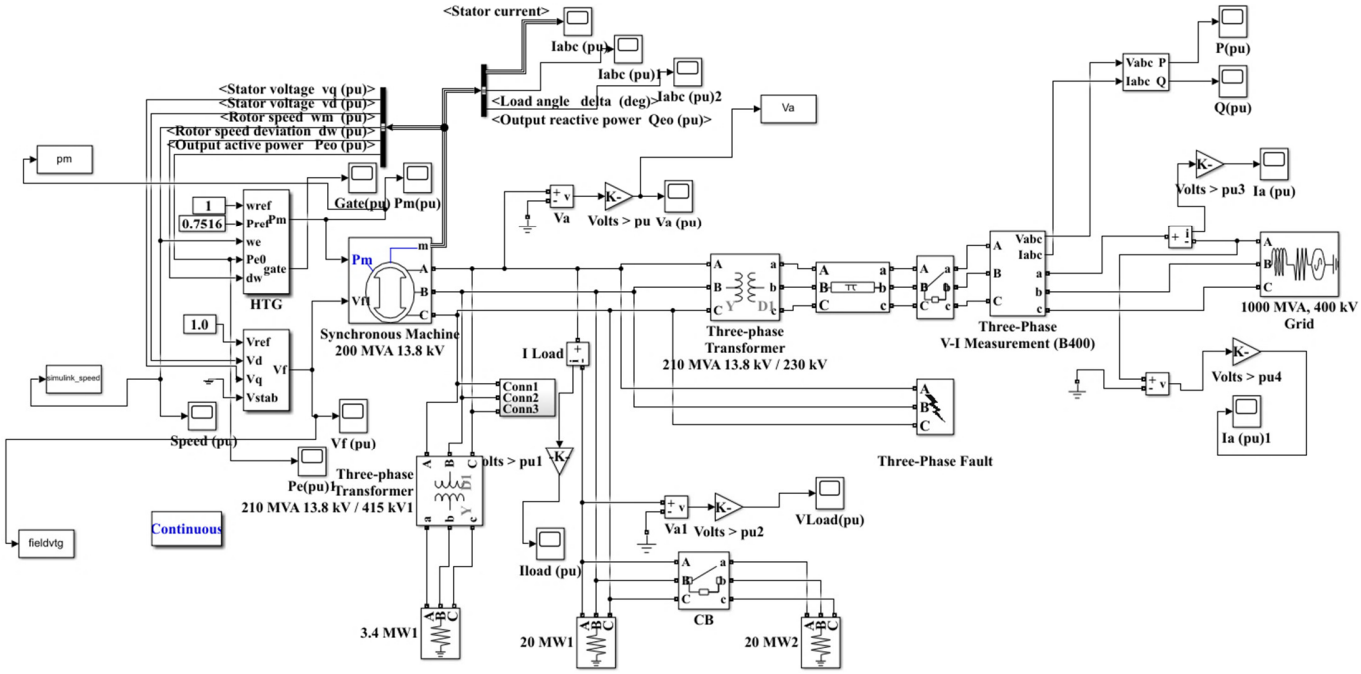

Fig. 3. MATLAB/Simulink model of the hydropower plant with a three-phase-to-ground fault scenario.

The PID governor and the automatic voltage regulator jointly ensured damping of oscillations and stability restoration. Performance metrics, such as rise time (around 0.5 s for voltage), settling time (about 1.5 s for speed), and limited overshoot (about 3%), confirm that the chosen control parameters are technically sound and align with industry practice. The controller gains were tuned to achieve fast damping and minimal overshoot, and their performance metrics closely match those reported in recent hydropower simulation studies [5, 8, 10, 14, 24, 25]. Unlike most previous models, which focused on generic governor or excitation configurations, the present model incorporates site-based validation and transient fault simulation, demonstrating realistic system recovery times consistent with reported industrial data. This practical validation reinforces the novelty and reliability of the proposed model for dynamic performance analysis of low-head hydropower plants.

The present study assumes ideal sensor feedback, a fixed resistive load, and a salient-pole synchronous generator, which is typical for low-speed hydroelectric units. This configuration accurately represents the rotor structure of the Nerinjipettai plant and is used consistently throughout all stages of the modeling process. Operational data from the Nerinjipettai plant were used to tune key parameters and validate the simulation model, ensuring realistic system dynamics. During the simulations, a slight delay in rotor speed stabilization was observed, primarily due to hydraulic inertia and servo-motor response lag, both of which are inherent to low-head hydropower systems.

Furthermore, the adopted modular MATLAB/Simulink framework provides greater flexibility for integrating hydraulic, electrical, and control subsystems than traditional transfer-function-based models do. The initial rotor speed and generator terminal voltage were set to their nominal operating values, and the unit was connected to a constant load. Although this approach helps focus on transient stability analysis, future work could incorporate seasonal water flow variability, measurement noise, and additional field measurements to further refine the model.

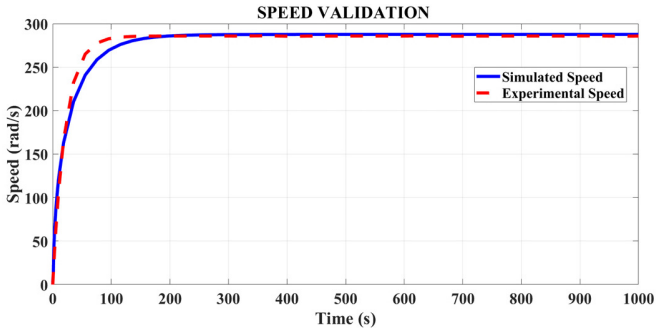

Fig. 4. Rotor speed response during the three-phase-to-ground fault.

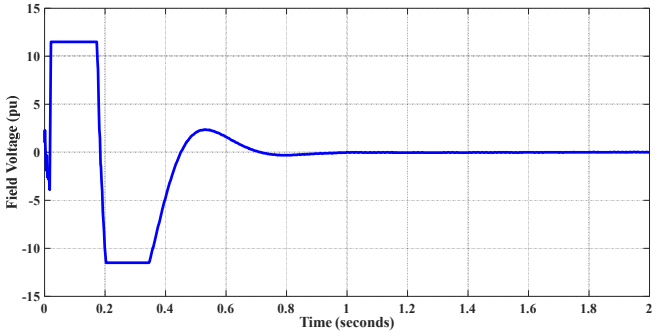

Fig. 5. Field voltage response during the three-phase-to-ground fault.

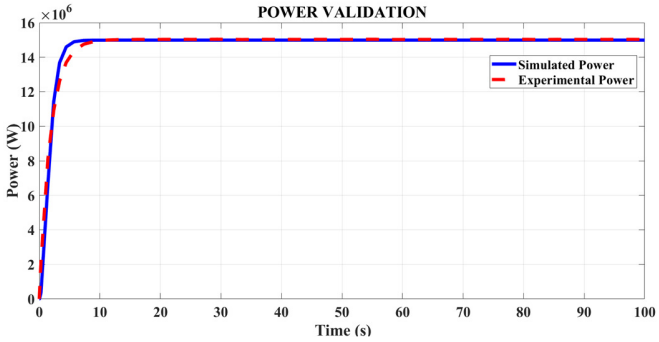

Fig. 6. Mechanical output power during the three-phase-to-ground fault.

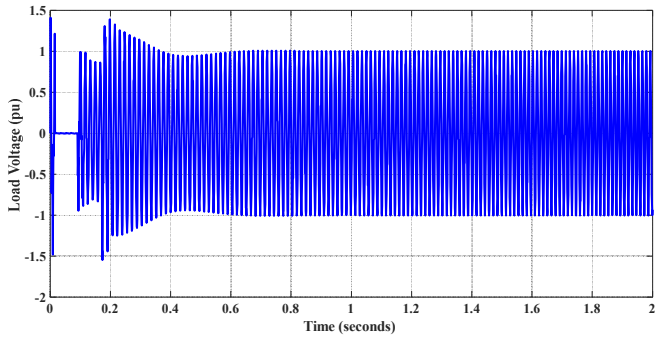

Fig. 7. Load voltage response during the three-phase-to-ground fault.

Potential sources of error in the model include variations in water temperature, pressure, and hydraulic inertia, which can influence turbine efficiency and response time. In practical plants, such factors, along with unmodeled disturbances in control loops, may slightly alter system transients. Although these were not explicitly simulated here, acknowledging them provides context for interpreting the presented results.

VI. CONCLUSION

The model developed to simulate hydroelectric power plants provides a good understanding of real-world dynamics, such as water flow, turbine gate opening, and sensitivity to plant performance. This is important for ensuring realistic results. Under simulated fault conditions, the rotor speed deviated by only about 2%, whereas the terminal voltage dipped by nearly 10% and recovered within 0.6 s, confirming effective transient stability. However, not every hydropower plant has the same characteristics or water availability, which limits the applicability of this model. Future work could incorporate seasonal water flow variations, hydrological uncertainties, and non-ideal sensor effects, making the model more adaptable to different sites. This would enable operators to consider their plant's unique characteristics and test concepts in real-world scenarios.

REFERENCES

[1] E. Helerea, M. D. Calin, and C. Musuroi, "Water Energy Nexus and Energy Transition—A Review," *Energies*, vol. 16, no. 4, Feb. 2023, Art. no. 1879, https://doi.org/10.3390/en16041879.

[2] Y. Zhang, H. Ma, and S. Zhao, "Assessment of hydropower sustainability: Review and modeling," *Journal of Cleaner Production*, vol. 321, Oct. 2021, Art. no. 128898, https://doi.org/10.1016/j.jclepro.2021.128898.

[3] I. P. Idoko, T. R. Ayodele, S. M. Abolarin, and D. R. E. Ewim, "Maximizing the cost effectiveness of electric power generation through the integration of distributed generators: wind, hydro and solar power," *Bulletin of the National Research Centre*, vol. 47, no. 1, Nov. 2023, Art. no. 166, https://doi.org/10.1186/s42269-023-01125-7.

[4] D. Altinbilek, K. Seelos, and R. Taylor, "Hydropower's Role in Delivering Sustainability," *Energy & Environment*, vol. 16, no. 5, pp. 815–824, Sept. 2005, https://doi.org/10.1260/095830505774478503.

[5] C. Chen, H. Liu, Y. Xiao, F. Zhu, L. Ding, and F. Yang, "Power Generation Scheduling for a Hydro-Wind-Solar Hybrid System: A Systematic Survey and Prospect," *Energies*, vol. 15, no. 22, Nov. 2022, Art. no. 8747, https://doi.org/10.3390/en15228747.

[6] C. G. Marcelino *et al.*, "An efficient multi-objective evolutionary approach for solving the operation of multi-reservoir system scheduling in hydro-power plants," *Expert Systems with Applications*, vol. 185, Dec. 2021, Art. no. 115638, https://doi.org/10.1016/j.eswa.2021.115638.

[7] R. Baniya *et al.*, "Nepal Himalaya offers considerable potential for pumped storage hydropower," *Sustainable Energy Technologies and Assessments*, vol. 60, Dec. 2023, Art. no. 103423, https://doi.org/10.1016/j.seta.2023.103423.

[8] G. Janevska, S. Panovski, and C. Dimitrieska, "Comparative Analysis of Mathematical Models of Penstock Dynamics at Hydropower Plants," *International Journal of Scientific & Engineering Research*, vol. 9, no. 10, pp. 652–657, Oct. 2018.

[9] A. Riasi, M. Raisee, and A. Nourbakhshv, "Simulation of Transient Flow in Hydroelectric Power Plants Using Unsteady Friction.," *Strojniški Vestnik - Journal of Mechanical Engineering*, vol. 56, no. 6, pp. 377–384, June 2010.

[10] W. Guo and D. Zhu, "A Review of the Transient Process and Control for a Hydropower Station with a Super Long Headrace Tunnel," *Energies*, vol. 11, no. 11, Nov. 2018, Art. no. 2994, https://doi.org/10.3390/en11112994.

[11] B. Xu *et al.*, "Modeling a pumped storage hydropower integrated to a hybrid power system with solar-wind power and its stability analysis," *Applied Energy*, vol. 248, pp. 446–462, Aug. 2019, https://doi.org/10.1016/j.apenergy.2019.04.125.

[12] D. A. Elalfy, E. Gouda, M. F. Kotb, V. Bureš, and B. E. Sedhom, "Comprehensive review of energy storage systems technologies, objectives, challenges, and future trends," *Energy Strategy Reviews*, vol. 54, July 2024, Art. no. 101482, https://doi.org/10.1016/j.esr.2024.101482.

[13] W. Yang *et al.*, "Pumped storage hydropower operation for supporting clean energy systems," *Nature Reviews Clean Technology*, vol. 1, no. 7, pp. 454–473, July 2025, https://doi.org/10.1038/s44359-025-00057-x.

[14] M. Masmali, M. I. Elimy, M. Fterich, E. Touti, and G. Abbas, "Comparative Studies on Load Frequency Control with Different Governors connected to Mini Hydro Power Plant via PSCAD Software," *Engineering, Technology & Applied Science Research*, vol. 14, no. 1, pp. 12975–12983, Feb. 2024, https://doi.org/10.48084/etasr.6722.

[15] S. Shandilya, S. P. Shelar, S. Prasad Das, D. Chatterjee, and R. P. Saini, "Performance evaluation of a bulb turbine designed for ultra-low head applications," *Journal of Physics: Conference Series*, vol. 1276, no. 1, Aug. 2019, Art. no. 012024, https://doi.org/10.1088/1742-6596/1276/1/012024.

[16] Z. Krzemianowski and M. Kaniecki, "Low-head high specific speed Kaplan turbine for small hydropower – design, CFD loss analysis and basic, cavitation and runaway investigations: A case study," *Energy Conversion and Management*, vol. 276, Jan. 2023, Art. no. 116558, https://doi.org/10.1016/j.enconman.2022.116558.

[17] W. Dong *et al.*, "A segmented optimal PID method to consider both regulation performance and damping characteristic of hydroelectric power system," *Renewable Energy*, vol. 207, pp. 1–12, May 2023, https://doi.org/10.1016/j.renene.2023.02.091.

[18] W. Ali, H. Farooq, A. Rasool, I. A. Sajjad, C. Zhenhua, and L. Ning, "Modeling and Analysis of the Dynamic Response of an Off-Grid Synchronous Generator Driven Micro Hydro Power System,"

International Journal of Renewable Energy Development, vol. 10, no. 2, pp. 373–384, May 2021, https://doi.org/10.14710/ijred.2021.33567.

[19] M. M. Rahimian and K. Butler-Purry, "Modeling of synchronous machines with damper windings for condition monitoring," in *2009 IEEE International Electric Machines and Drives Conference*, Miami, FL, USA, 2009, pp. 577–584, https://doi.org/10.1109/IEMDC.2009.5075264.

[20] A. Demiroren and H. L. Zeynelgil, "Modelling and Simulation of Synchronous Machine Transient Analysis Using Simulink," *International Journal of Electrical Engineering & Education*, vol. 39, no. 4, pp. 337–346, Oct. 2002, https://doi.org/10.7227/IJEEE.39.4.4.

[21] S. C. Chapra and R. Canale, *Numerical Methods for Engineers*, 8th ed. New York, NY, USA: McGraw-Hill, 2005.

[22] J. Tiwari, A. K. Singh, A. Yadav, and R. K. Jha, "Modelling and Simulation of Hydro Power Plant using MATLAB & WatPro 3.0," *International Journal of Intelligent Systems and Applications*, vol. 7, no. 8, pp. 1–8, July 2015, https://doi.org/10.5815/ijisa.2015.08.01.

[23] J. C. Boemer, M. Gibescu, and W. L. Kling, "Dynamic models for transient stability analysis of transmission and distribution systems with distributed generation: An overview," in *2009 IEEE Bucharest PowerTech*, Bucharest, Romania, 2009, pp. 1–8, https://doi.org/10.1109/PTC.2009.5282177.

[24] F. Fallahi, M. Yildirim, S. Zhao, and F. Qiu, "A Sensor-Driven Optimization Framework for Asset Management in Energy Systems: Implications for Full and Partial Digital Transformation in Hydro Fleets." arXiv, Apr. 21, 2025, https://doi.org/10.48550/arXiv.2504.15483.

[25] J. Pearce, A. Khojaste, G. Zakeri, and G. Pritchard, "Baseline hydropower generation offer curves." arXiv, Aug. 06, 2025, https://doi.org/10.48550/arXiv.2508.04854.